

PLEASE DO NOT REMOVE FROM LIBRARY

RI 9004

Bureau of Mines Report of Investigations/1986

Evaluation of a Ground Penetrating Radar System for Detecting Subsurface Anomalies

By Ronald H. Church and William E. Webb



UNITED STATES DEPARTMENT OF THE INTERIOR

RI 9004

Report of Investigations 9004

Evaluation of a Ground Penetrating Radar System for Detecting Subsurface Anomalies

By Ronald H. Church and William E. Webb



UNITED STATES DEPARTMENT OF THE INTERIOR
Donald Paul Hodel, Secretary

BUREAU OF MINES
Robert C. Horton, Director

This research at the Tuscaloosa Research Center was carried out under an agreement between the Bureau of Mines, U.S. Department of the Interior, and the Florida Institute of Phosphate Research.

Library of Congress Cataloging in Publication Data :

Church, Ronald H

Evaluation of a ground penetrating radar system for detecting subsurface anomalies.

(Report of investigations / United States Department of the Interior, Bureau of Mines ; 9004)

Bibliography: p. 21.

Supt. of Docs. no.: I 28.23: 9004.

1. Sinkholes--Florida. 2. Ground penetrating radar. 3. Dam failures--Florida. I. Webb, William E. II. Title. III. Series: Report of investigations (United States. Bureau of Mines) ; 9004.

TN23.U43 [GB600.3.F56] 622s [55 1.4'47] 85-600243

CONTENTS

	<u>Page</u>
Abstract.....	1
Introduction.....	2
Acknowledgments.....	3
GPR system requirements.....	3
Development of a propagation model.....	5
Radar range equation.....	5
Detection gain.....	7
Implementation loss.....	7
Minimum detectable power.....	7
Signal and noise ratios.....	7
Discussion of model results.....	7
Subsurface GPR probe.....	8
Borehole probe specifications.....	8
Surface control unit specifications.....	8
System operation.....	10
Subsurface GPR test.....	10
Image enhancement.....	14
Surface GPR unit.....	15
Surface GPR test.....	16
Surface damsite test.....	20
Conclusions.....	20
References.....	21

ILLUSTRATIONS

1. Plot of holes drilled at the Mulberry, FL, site.....	4
2. Log of hole H depicting differing strata.....	4
3. Propagation path of radar waves.....	6
4. Block diagram detailing major elements of GPR subsurface probe system.....	9
5. Surface control unit with computer console, disk drive, and storage oscilloscope.....	11
6. Borehole radar probe assembly and major divisions.....	11
7. Block diagram detailing circuitry in each major division of borehole probe	11
8. GPR subsurface probe assembly being set up over hole G.....	12
9. GPR subsurface probe being lowered to a depth of 45 ft.....	12
10. Surface control unit and computer console taking data during scan.....	13
11. Correlation of signatures obtained in hole H.....	13
12. Exploded view of radar signatures at the 63- to 71-ft depth.....	14
13. Schematic of the surface transmitter.....	15
14. Schematic of 4,000-W, 1,200-V power supply.....	16
15. Transmitter attached to surface dipole antenna.....	17
16. Control console, with built-in power supply, during a field demonstration.	17
17. Radar scans.....	18
18. Log of solid-ground hole approximately 1,000 ft north of cavity.....	19

TABLES

1. Typical overburden strata thickness and composition from cored hole.....	5
2. Electrical properties of overburden.....	5
3. Summary of propagation losses.....	7

UNIT OF MEASURE ABBREVIATIONS USED IN THIS REPORT

dB	decibel	lb/in ²	pound per square inch
dB/ns	decibel per nanosecond	μF	microfarad
dB•W	decibel-watt	μH	microhenry
ft	feet	MHz	megahertz
ft/ns	feet per nanosecond	min	minute
ft/s	feet per second	ns	nanosecond
Hz	hertz	Ω	ohm
in	inch	pct	percent
kHz	kilohertz	pF	picofarad
kΩ	kilohm	V	volt
kW	kilowatt	W	watt
lb	pound		

EVALUATION OF A GROUND PENETRATING RADAR SYSTEM FOR DETECTING SUBSURFACE ANOMALIES

By Ronald H. Church¹ and William E. Webb²

ABSTRACT

The Bureau of Mines tested a ground penetrating radar (GPR) system in the central Florida phosphate district to determine the feasibility of utilizing GPR technology for subsurface cavity detection.

The test area is located in karst topography where sinkhole development is prevalent. State regulations require subsurface drilling of damsites to identify underground anomalies; however, this method is not totally accurate in locating subsurface cavities that could lead to sinkhole development. An electromagnetic method of identifying anomalous subsurface conditions could reduce or eliminate the possibility of dam failure due to sinkhole development.

The Bureau devised a GPR system that successfully penetrated over 50 ft of overburden and gave recognizable radar return signals characteristic of a rock-cavity interface.

¹Mining engineer, Tuscaloosa Research Center, Bureau of Mines, Tuscaloosa, AL.

²Electrical engineer (faculty), Tuscaloosa Research Center.

INTRODUCTION

Approximately 75,000 acres of phosphate settling areas exist in the central Florida phosphate area. Each year about 4,000 acres of new settling areas, requiring 38 miles of new dams, are constructed. Although no dam failure has been attributed to sinkhole formation, State regulations require the identification of subsurface conditions that could lead to dam failure. Section 17-9 of the Florida Administrative Code provides guidelines for damsite evaluation. Compliance with these guidelines requires that a drilling program be implemented for the evaluation of a site for dam construction.

In drilling a proposed damsite on approximately 500-ft centers, the probability of detecting a cavity 50 ft wide by 50 ft long is 1 in 100. Achieving a 50-pct probability of hitting this cavity would require 50 holes. Since cost estimates for drilling 100-ft exploratory holes range from \$350 to \$400 per hole, it becomes evident that a more accurate and economical method should be identified to reduce even further the potential for dam failure due to sinkhole development. The purpose of this Bureau of Mines investigation was to determine the feasibility of using GPR as an additional tool in subsurface cavity detection.

GPR systems have been developed for many applications in the mining industry. GPR's have been used in geological exploration (1-3),³ where recognizable radar return signatures were obtained through 130 ft of dolomite and 900 ft of granite. In salt domes, where radiofrequency (RF) attenuation is much lower, discontinuities were detected at 2,000 to 3,200 ft.

Bureau of Mines research has included work with microwave radars used for the delineation of coal seams (thickness, shape, and orientation) (4-5). XADAR Corp.⁴ developed a short-pulse GPR for the Bureau which was capable of

penetrating 100 ft in a coal seam (6-8) where voids were detectable at 50 ft using a frequency of 10 to 160 MHz. In another test, an uncased borehole was detected through 25 ft of coal. These results were significant in that the conductivity of coal is high, which results in poor propagation of electromagnetic (EM) waves.

A borehole probe-type radar was developed by Bureau of Mines contractors (9-10). With this unit, utilizing a combination receiver-transmitter probe, two-way penetration was limited to 50 ft.

Another Bureau contractor developed separate transmitter and receiver probes (11-12). These probes were lowered through boreholes on each side of a tunnel. The signal propagated through 30 ft of material and successfully located the tunnel but was unable to determine its size accurately.

The Bureau also devised a GPR for use in mine strata control. This unit was designed to operate at high frequencies to permit higher resolution at the expense of signal propagation. Recognizable return radar signatures characteristic of the roof strata were obtained through approximately 8 ft of mine roof. The upper coal seam, overlying the immediate roof, was mapped along with the main roof. Signal interpretation was difficult because of the manifold anomalous conditions encountered. These gave several lesser returns, which required computer analysis for interpretation.

A Bureau-designed synthetic pulse radar system was tested in 1981. The penetration distance was approximately two times greater than that of the short-pulse GPR (13). One test site, at a mine in Utah, gave reflection depths of 40 ft where the background noise was found to be 60 dB lower than the strength of the main signal. For this area, estimates of approximately 200 ft for maximum signal propagation have been made.

³Underlined numbers in parentheses refer to items in the list of references at the end of this report.

⁴Reference to specific products does not imply endorsement by the Bureau of Mines.

ACKNOWLEDGMENTS

The authors wish to express their appreciation to the Florida Institute of Phosphate Research (FIPR) for its cooperation and cofunding in this research effort to develop a GPR for subsurface anomaly detection.

International Minerals and Chemical Corp.'s assistance in site selection and preparation is also acknowledged, as is the Florida Bureau of Geology for its counsel in geological interpretation of the subsurface at the sites and its drilling of the test holes.

GPR SYSTEM REQUIREMENTS

In the initial phase of the research, test site requirements were established. It was determined that a suitable test cavity should be located in the central Florida phosphate district, this being the predominant area for sinkhole formation. It should lie 50 to 100 ft below the surface, i.e., at the drilling depth the phosphate industry reaches in its tests to determine subsurface integrity. For test purposes it was determined that a cavity should be at least 10 ft wide and 5 to 10 ft thick to serve as a reliable target. Several mining companies and government agencies were contacted in this phase of the project. Drilling logs from mining companies and the U.S. Geological Survey were reviewed.

Two sites were selected that met the established criteria. The first site, located in Hillsborough County (section 23, township 32 south, range 21 east), had been previously drilled by International Minerals and Chemical Corp. (IMC). A second site was located in Polk County (section 32, township 29 south, range 23 east) near Mulberry. This site also was located on IMC property. The cavity had been detected by previous drilling 58 ft below the surface. Evidence of the drilling site was still visible, so the initial Bureau of Mines test hole at this site was drilled alongside the hole previously drilled. The cavity was intersected approximately 58 ft below the

surface and had a vertical void dimension of 10 ft. The first (or top) 3 ft of the cavity was water filled, the next 4 ft contained a turbid mixture of water and clay, and the last 3 ft was comprised of a compacted clay layer.

As shown in figure 1, a grid consisting of nine holes was drilled to delineate the boundaries of the cavity. Holes A, B, E, F, and I intersected the cavity approximately 60 ft below the surface. Holes C, D, G, and H were drilled into solid ground to a depth of approximately 80 ft. As shown in figure 1, the cavity dimension was between 100 and 200 ft in the north-south direction and between 50 and 100 ft in the east-west direction. This, however, can be misleading since the cavity is probably very irregular in shape. The cavity was intersected at depths ranging from 56 to 63 ft with the void averaging 10 to 11 ft in thickness.

An open casing using 4-in polyvinyl chloride (PVC) pipe was installed in hole A to a depth of 55 ft, which was identified as the top of the limestone overlying the cavity. Holes C, D, H, and G were cased to their bottom. The core of hole H was characterized to identify the subsurface lithology (fig. 2) through which the radar waves passed. These holes were selected to be the test holes for the subsurface probe. The remaining holes, which intersected the cavity, were plugged.

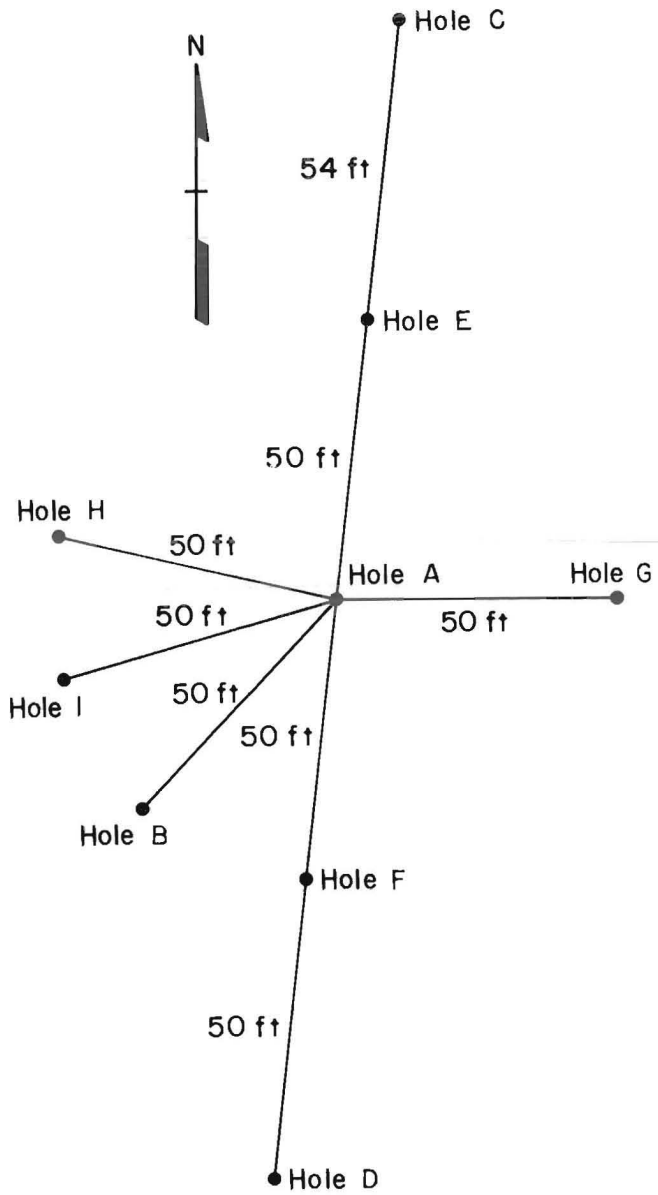


FIGURE 1. - Plot of holes drilled at the Mulberry, FL, site.

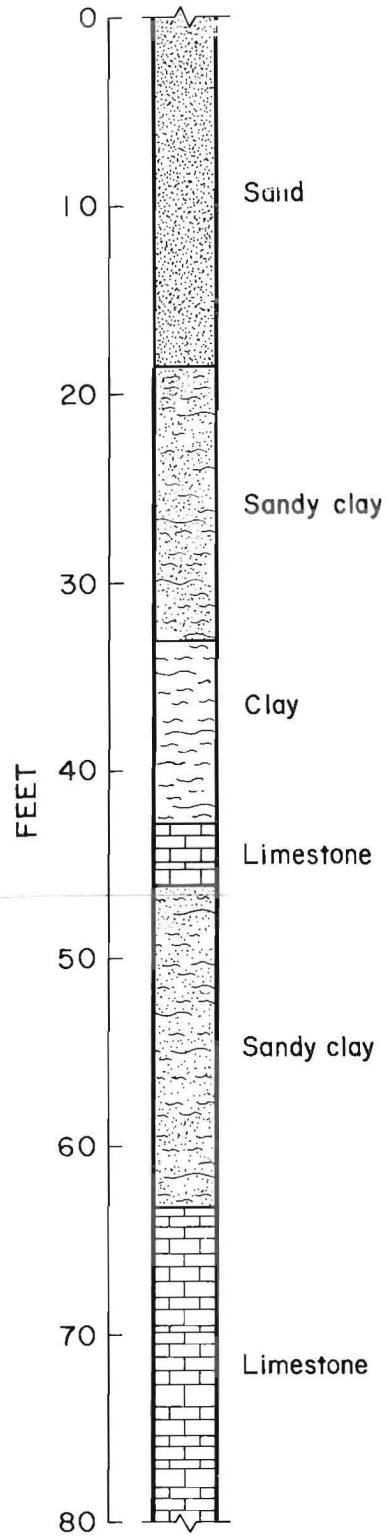


FIGURE 2. - Log of hole H depicting differing strata. The top of the cavity lies at approximately 58 ft.

DEVELOPMENT OF A PROPAGATION MODEL

The core sample was used to determine the lithology (table 1) of the rock and soil overlying the cavity. This lithology was found to be generally typical of the subsurface materials found in the central Florida phosphate district. The relative permeativity and loss tangent were measured for the limestone stratum over a frequency range of 100 to 1,000 MHz and were found to be relatively independent of frequency over this range. The values for the other strata (sand and clay) were taken from published values (14). The top stratum was assumed to be relatively dry sand (10 pct moisture). The clay stratum was assumed to be water saturated. No data were available for sandy clay, so an average was assumed from the published values for water-saturated sand and clay; these data represent the worst case scenario. Table 1 is a classification of the individual strata of the overburden material compiled from the cored hole data shown in figure 2. The electrical properties for this overburden are shown in table 2 (14). The attenuation constant and losses in each strata were calculated using

the methodology presented in the next section. These values are also shown in table 2.

RADAR RANGE EQUATION

The power at the receiving antenna (P_R) is given by

$$P_R = P_T - L_T, \quad (1)$$

where P_T is the transmitted power and L_T is the total loss between the transmitter and receiver. The transmitted and received power are expressed in dB·W and the loss in dB. The total loss can be written as

$$L_T = L_b + L_p + L_t - G_R - G_T. \quad (2)$$

Here L_b is the propagation loss for two ideal isotropic antennas in free space, L_p is the path loss which accounts for attenuation and scattering over the actual path, L_t is the loss due to reflection at the target (in this case the upper surface of the cavity), and G_R and G_T are the receiver and transmitter antenna gains.

TABLE 1. - Typical overburden strata thickness and composition from cored hole

Strata	Depth, ft	Thickness, ft	Material
1.....	0-17	17	Relatively dry sand.
2.....	17-31	14	Saturated sandy clay.
3.....	31-42	11	Saturated clay.
4.....	42-45	3	Limestone.
5.....	45-55	10	Saturated sandy clay.
6.....	55-58	3	Limestone.
7.....	>58	NAP	Water-filled cavity (detected in hole A).

NAP Not applicable.

TABLE 2. - Electrical properties of overburden

Strata	Relative permeativity (ϵ_r)	Loss tangent ($\tan \delta$)	Attenuation constant, (α), m^{-1}	Loss, dB	
				Attenuation	Reflection
1.....	2.5	0.026	3.3×10^{-2}	1.57	0.8
2.....	15.0	.20	4.2×10^{-2}	1.64	.02
3.....	11.0	.25	7.1×10^{-2}	2.16	.05
4.....	7.0	2.9×10^{-4}	1.3×10^{-4}	.001	.16
5.....	15.0	.20	4.2×10^{-2}	2.16	.16
6.....	7.0	2.9×10^{-4}	1.3×10^{-4}	.001	NAP

NAP Not applicable.

If it is assumed that the top of the cavity is a plane horizontal surface whose extent is large compared to the dimensions of the antenna, the transmitting antenna can then be replaced by its image formed by the reflection of the wave from the upper surface of the cavity, as shown in figure 3. The free space propagation loss is then given by (15)

$$L_b = 10 \log \left(\frac{4\pi l}{\lambda} \right)^2, \quad (3)$$

where l is twice the cavity depth (d) and λ is the wavelength. Note that this geometry leads to a propagation loss that is proportional to the square of the target distance, whereas the usual radar range equation contains the fourth power of this quantity. This is due to the fact that the usual radar range equation applies to a distant target that is small compared to the cross-sectional area of the transmitted beam.

The path loss L_p consists of two parts: the loss due to absorption in each strata of the overburden, and the loss due to reflection at the interfaces between strata types. The absorption in the i -th strata of thickness X_i is

$$L'_i = 10 \log (e^{-\alpha_i X_i}), \quad (4)$$

where α_i is the absorption coefficient of the material of strata type i . The absorption coefficient can be calculated from the relative permeability ϵ_r and loss tangent ($\tan\delta$) by the relation

$$\alpha_i = \frac{\pi f \sqrt{\epsilon_{r_i}} \tan\delta_i}{c}, \quad (5)$$

where f is the frequency, i is the individual strata type, and c is the speed of light.

The loss due to reflection at the interface of the strata between the i and $i+1$ strata can be derived from Fresnel's equation,

$$\left| \frac{E_r}{E_i} \right| = \left| \frac{\eta_i - \eta_{i+1} + 1}{\eta_i + \eta_{i+1} + 1} \right|. \quad (6)$$

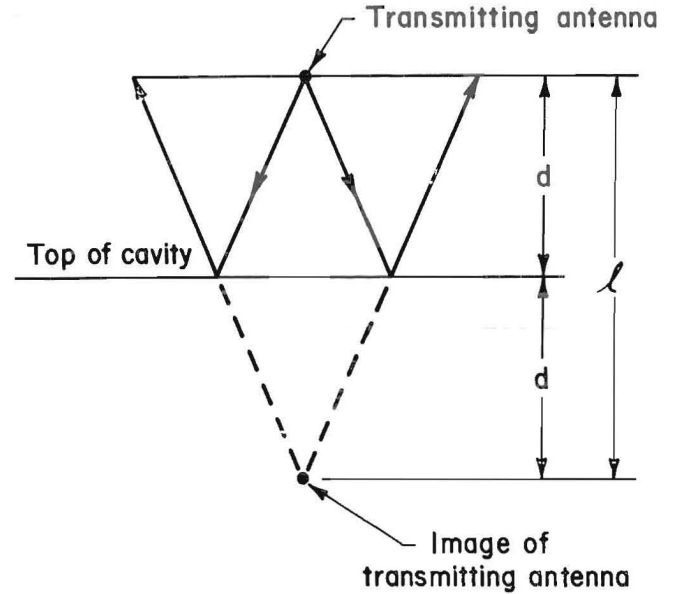


FIGURE 3. - Propagation path of radar waves.

Here η_i is the intrinsic impedance of the i -th strata and is given by

$$\eta_i = \frac{\sqrt{\mu_i}}{\sqrt{\epsilon_{r_i}}}. \quad (7)$$

Also, if it is assumed that the permeabilities (μ_i) are the same for all strata, then the loss due to reflection L''_i can be written as

$$L''_i = 10 \log \left(1 - \left| \frac{E_r}{E_i} \right|^2 \right) \quad (8)$$

$$L''_i = 10 \log \left(1 - \left(\frac{\sqrt{(1 - \epsilon_{r_i})(\epsilon_{r_i} - 1)}}{\sqrt{(1 + \epsilon_{r_i})(\epsilon_{r_i} + 1)}} \right)^2 \right) \quad (9)$$

and the total path loss becomes

$$L_p = 2 \sum L'_i + 2 \sum L''_i. \quad (10)$$

The factor of 2 appears in equation 10 because each layer is transversed twice.

The target loss L_t may be calculated by applying Fresnel's equation to the boundary between the lowest stratum in the overburden and the material filling the cavity. For these calculations it is assumed that the cavity is water filled.

The gain of a half-wave dipole (i.e., 1.64 dB at each antenna) has been assumed as the antenna gain.

DETECTION GAIN

The GPR averages any number of pulses to produce the final signal. The number of pulses averaged can be set from the computer console. Averaging n pulses increases the signal-to-noise ratio by the square root of n , which is equivalent to a gain of $5 \log(n)$, which may be subtracted from the total loss. For these calculations it was assumed that 20 pulses would be averaged so that the detection gain would be 6.5 dB.

IMPLEMENTATION LOSS

Radar systems seldom perform as well as feasibility calculations indicate they should. This is due to a number of small effects (such as imperfect impedance matching to the antenna) that tend to degrade system performance. For the development of this propagation model, an additional 6 dB has been added to the total losses as is customary to allow for these effects.

MINIMUM DETECTABLE POWER

The minimum signal power required at the receiver was determined by operating the radar in an area where no target was present. The observed return signal was assumed to be a result of thermal noise in the receiver, atmospheric noise, electromagnetic interference, backscatter from the earth, etc. The effective noise power into the receiving antenna was then calculated from the magnitude of this signal and was found to range from -38 to -48 dB·W. The relatively large range observed was attributed to the fact that

most of the receiver noise was caused by backscatter from the heterogeneity of the earth surface and material and was therefore dependent on the location of the antenna.

SIGNAL AND NOISE RATIOS

The receiver signal-to-noise ratio was calculated by subtracting the total loss from the transmitted power to obtain the received power due to reflection from the cavity. The signal-to-noise ratio is then the difference in the received signal power and the receiver noise power. These calculations are summarized in table 3.

TABLE 3. - Summary of propagation losses

Transmitter power.....dB·W..	40
Propagation loss.....dB..	<u>53.59</u>
Path loss:	
Attenuation.....dB..	15.06
Reflection at strata.....dB..	<u>2.38</u>
Total.....dB..	17.44
Target loss.....dB..	5.30
Antenna gain.....dB..	-3.28
Detection gain.....dB..	-6.5
Implementation loss.....dB..	6.0
Total loss.....dB..	72.55
Receiver power.....dB·W..	-32.55
Minimum detectable	
power.....dB·W..	-38 to -48
Signal margin.....dB..	+6 to -16

DISCUSSION OF MODEL RESULTS

The propagation calculations for the GPR indicated that the reflection from a water-filled cavity 62 ft below the surface could be expected to be 6 to 16 dB above the background noise. This corresponded to a factor of 2 to 6 in the output signal. Although these values were marginal in terms of detectability, they still indicated that there would be a reasonable chance of detecting the cavity.

SUBSURFACE GPR PROBE

The probe used for the subsurface tests for detecting cavities was developed and tested for the Bureau during the late 1970's and early 1980's. This GPR system was constructed by Southwest Research Institute for the Bureau and was designed to detect subsurface cavities and other anomalous features from a borehole drilled from the surface. The system is composed of a high-power transmitter, a directional antenna rotation mechanism, and a sensitive broadband signal receiver. The GPR is divided into two main parts, a surface control unit and a subsurface probe assembly. The surface unit has the capability of controlling all probe functions including receiver gain, receiver sampling rate, antenna position, and power control. The subsurface probe contains the antenna assembly, transmitter, power supply, and circuitry necessary to complete a two-way communications link.

The first field demonstration of the GPR probe utilized a very-high-frequency (VHF) video-pulse radar. Previous borehole radar tests of this unit in a faulted area identified a coal-rock interface at a distance of 40 ft (16). Borehole-to-borehole tests with a separate receiver and transmitter obtained distances up to 175 ft between boreholes, and the GPR was capable of penetrating through a coal seam. The coal seam was indicated by the GPR to be continuous, although previously thought to be completely separated by the fault.

This probe was modified following a series of tests conducted in November 1977 at Silver Spring, MD, by the developer, where underground subway structures were identified from a nearby borehole. A reflected signal was observed from a structure located approximately 60 ft from the probe for a total traveled distance of 120 ft. The Bureau's probe assembly was modified to include direction capabilities from its present omnidirectional response.

The electrical and mechanical specifications for the subsurface GPR system are described in the following tabulations by the basic functions of each subassembly (17).

BOREHOLE PROBE SPECIFICATIONS

Radar Transmitter

Probe repetition frequency.....kHz..	300
Power output.....kW..	1
Pulse width.....ns..	10

Radar Receiver

Noise figure (approx)..... dB..	3
Bandwidth.....MHz..	30-300
RF gain.....dB..	0 or 30
Time domain sampler window	
	ns.. 500
Sample pulse width.....ns..	1
Sampler output time base...Hz..	0.2 or 20

Antennas

Transmitter: Phased dual-dipole array; 18-dB front-to-back ratio directivity; mechanical positioning at eight preset rotational positions.

Receiver: Electrically short monopole, omnidirectional.

Mechanical

Length (without centralizers)..ft..	13.3
Diameter.....in..	3.0
Centralizers, upper length.....in..	20.75
Centralizers, lower length.....in..	19.5
Borehole diameter range.....in..	4-6
Total probe weight.....lb..	108
Cable head, 4-conductor, Gearhart-Owen.....in..	1.0
Pressure limit.....lb/in ² ..	500

SURFACE CONTROL UNIT SPECIFICATIONS

Electrical

Power: 115 V ac, 60 Hz.

Controls:

Antenna position, adjustable in 45° segments.

Antenna control, automatic or manual.

Borehole orientation, horizontal and/or vertical.

Electrical--Continued

Mechanical

Controls--Continued

Receiver gain:

- RF: High 30 dB, low 0 dB.
- Early: 0, 20, 40, or 60 dB.
- Display rate: 0.2 or 20 Hz.
- TVG range: 0, 0.1, 0.2, or 0.5 dB/ns.

Outputs:

- Video out, analog signal.
- Sync out, analog signal.
- Antenna position, digital.
- Display rate, digital.
- Antenna control, digital.
- RF gain, digital.
- Borehole orientation, digital.
- Early gain, digital.
- Gain slope, digital.

Control module size (standard module, width).....in..	4
Control module weight.....lb..	4.75
Power supply size (standard module, width).....in..	4
Power supply weight.....lb..	18.25
Cabinet size (standard rack-mountable bin with power supplies).....in..	19
Cabinet weight.....lb..	33

Figure 4 is a system diagram detailing the major elements of the system.

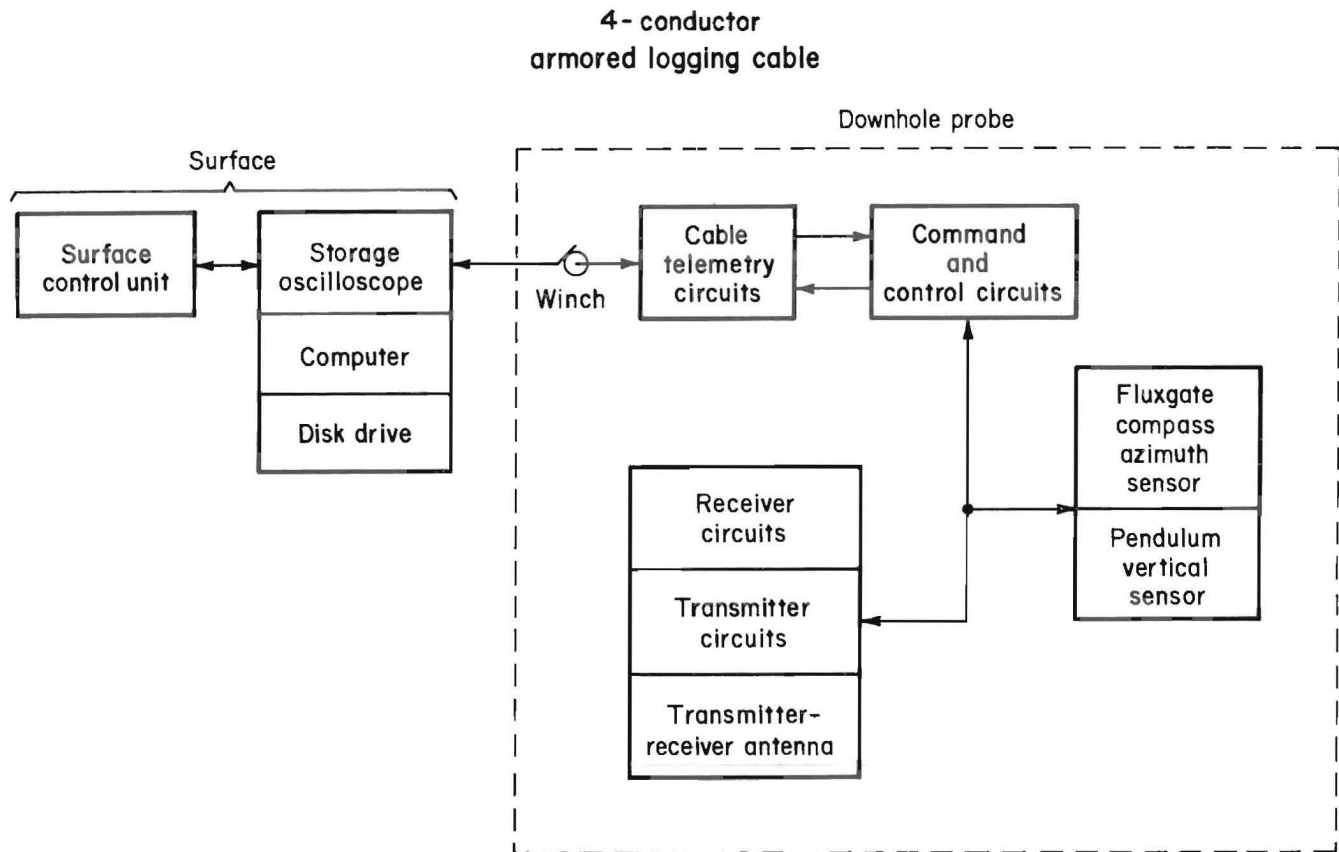


FIGURE 4. - Block diagram detailing major elements of GPR subsurface probe system.

SYSTEM OPERATION

The surface unit provided for command of all probe functions. Figure 5 shows the surface unit (top), disk drive (center), and computer and storage oscilloscope (bottom). Signals were received from the probe by a two-way communication link (four-conductor logging cable). Gain control, antenna positions, and display rate were also controlled by the surface unit. A synchronizing pulse from the transmitter, which indicates the start of the video waveform, was passed onto the receiver. Two gain control amplifiers (step gain and time-varying gain) permitted signal compensation for various degrees of electromagnetic signal attenuation.

The received signal was displayed on a storage oscilloscope. The voltage sensitivity and time base could then be set for maximum signal enhancement. The received data were then transferred to a magnetic data tape or floppy disk for later retrieval and data analysis. A computer was used for overall system operation and data acquisition. The cathode ray tube (CRT) displayed the received digital signal from the oscilloscope. This provided the operator with a "quick

look" analysis of the data and system performance prior to data storage.

As shown in figure 4, all operations for the receiver circuit, transmitter circuit, and antenna operations were located in the downhole probe unit. The probe was capable of direction finding in the vertical or horizontal position. This control was located on the surface unit. In the vertical position a flux-gate compass azimuth sensor was capable of searching and locking on any of eight antenna positions (0° to 315°). A scan mode was also possible for rapid search of easily recognizable signals. The power supply for the transmitter (1,000 W) was located in the probe assembly. Power was fed to the transmitter and trigger pulse generator, which radiates by means of four dipole antennas. The synchronizing antenna, when irradiated, told the surface unit to start the scan. The repetition rate of the pulse generator was 300 kHz. The receiver and antenna were also located in the probe housing. The receiver had a fixed sampling window of 500 ns, which represented approximately 500 ft of propagation in air (250 ft out and 250 ft back). Through sand, with 4 pct moisture and a dielectric constant of 5 (16), this represented a total window of between 200 and 250 ft. Figures 6 and 7 are detailed sketches of the probe and major systems. Notice the division of circuitry which allowed segregation of the antennas in the radome housing from the other circuitry.

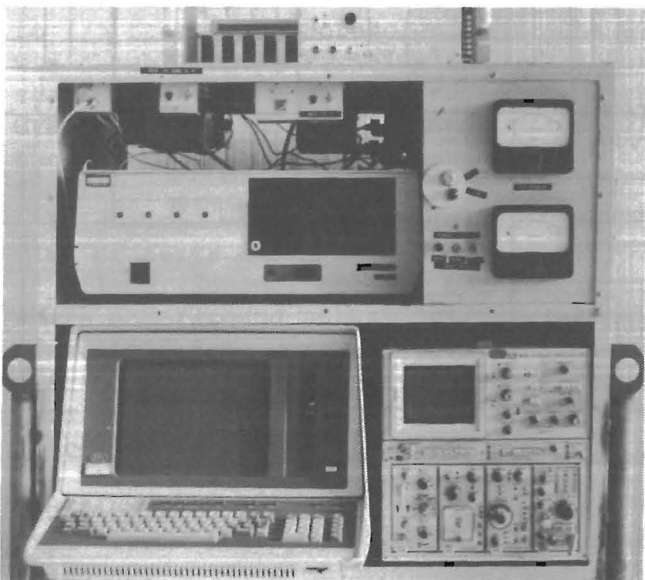


FIGURE 5. - Surface control unit with computer console, disk drive, and storage oscilloscope.

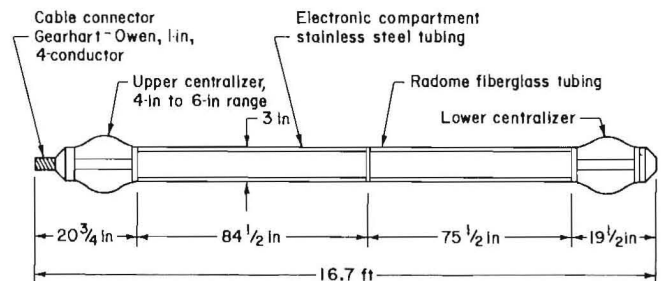


FIGURE 6. - Borehole radar probe assembly and major divisions.

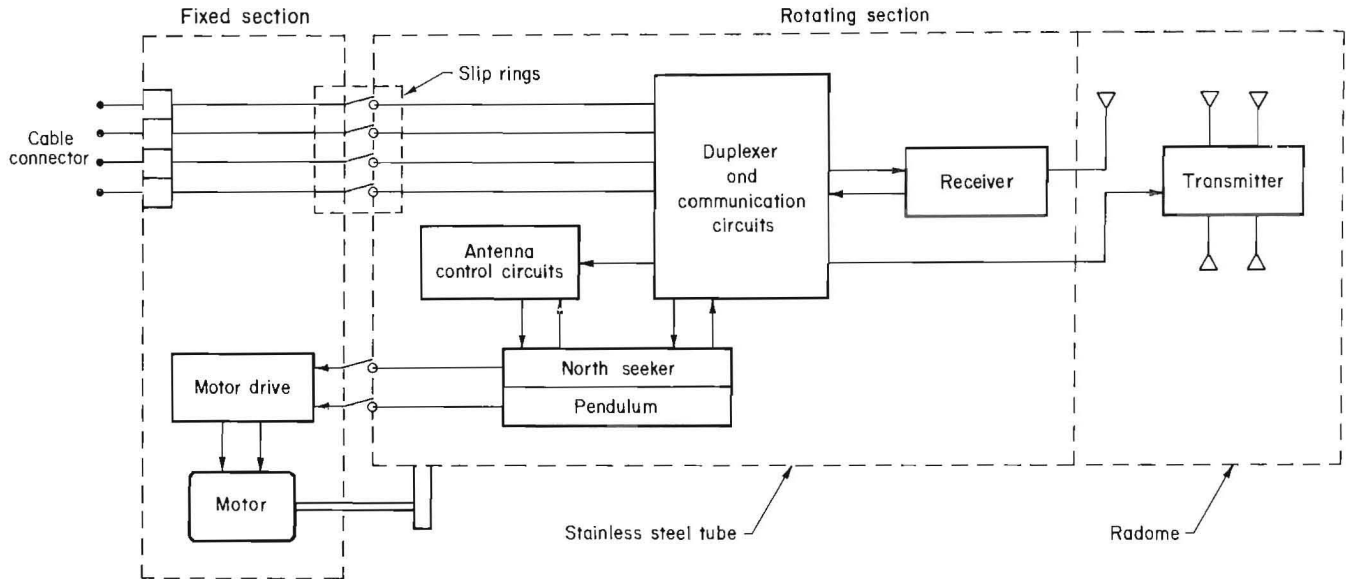


FIGURE 7. - Block diagram detailing circuitry in each major division of borehole probe.

SUBSURFACE GPR TEST

In April 1984, the GPR was taken to the Mulberry, FL, site for field demonstration. The probe was deployed at hole G, utilizing a modified trailer with a 20-ft boom for probe handling; figure 8 shows the probe unit being hoisted over the hole. The probe was then lowered (fig. 9) to a depth of 45 ft, approximately 13 ft above the top of the cavity. Readings were taken at 45° intervals, beginning due north. Figure 10 shows the surface control unit with auxiliary equipment during a test sequence. The probe was lowered in 2-ft increments to a depth of 73 ft, approximately 5 ft below the bottom of the cavity. At each level, two readings were taken at each of eight 45°

intervals. One reading was taken with an early gain setting and the other with a late gain setting, while utilizing differing time-varying gains. This allowed compensation for electromagnetic signal attenuation.

Following completion of tests at hole G, the unit was positioned at hole H and the sequence was repeated. The data, which were collected on magnetic tape, were analyzed for recognizable signatures. From a preliminary analysis of the test data, it was observed that late gain control did little to aid in signal reception. Performance seemed to be improved by utilizing an early gain setting.



FIGURE 8. - GPR subsurface probe assembly being set up over hole G.

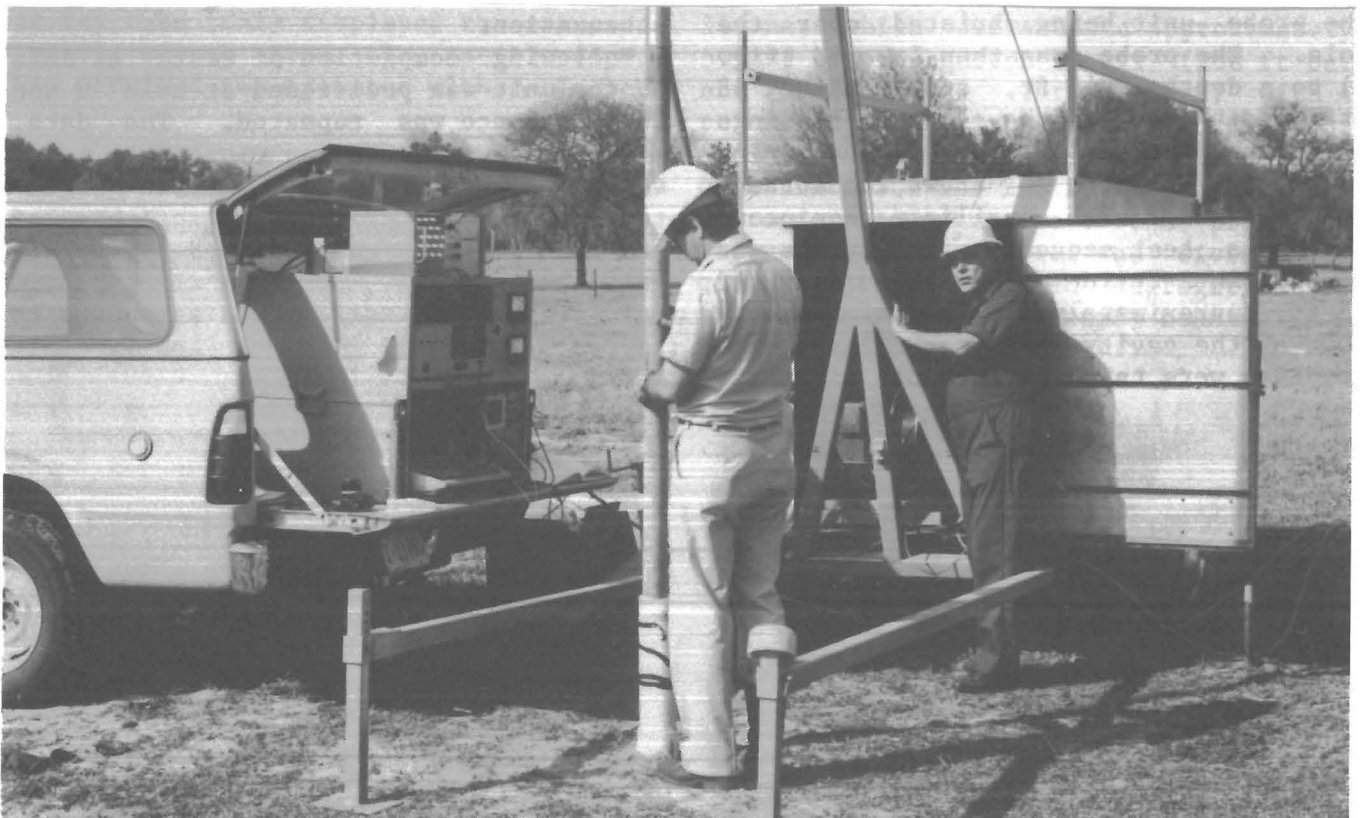


FIGURE 9. - GPR subsurface probe being lowered to a depth of 45 ft.

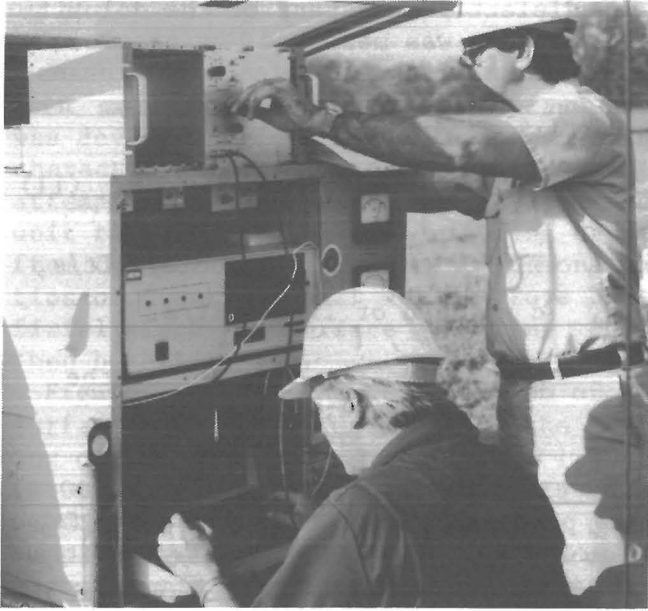


FIGURE 10. - Surface control unit and computer console taking data during scan.

From the data collected at hole G, located within 50 ft of cavity hole A, no recognizable radar signatures were identified that would indicate a cavity. However, recognizable signatures of cavity interception were obtained from the data of hole H. A total of 107 readings were taken in hole H, which was drilled within 25 ft of cavity hole I. Figure 11 is a graphic representation of the correlated computer-compiled data collected from hole H. In this figure the borehole log data (left) are compared to the radar data (right) taken at the depths indicated. These scans were taken in the southeast direction from hole H looking toward the cavity intersected by holes E, A, I, B, and F (fig. 1). The penetration depth of the signal through the strata is listed as the horizontal component. Note the reflections (fig. 11) seen at 80 ns horizontally into the strata at the 63- through 71-ft elevations. Figure 12 gives an enlarged view of these scans (63- to 71-ft depths). The general appearance of the waveform is that of an attenuated sine wave (idealized "text book" image), which would be expected of EM waves propagating through a homogeneous medium. These waves would be

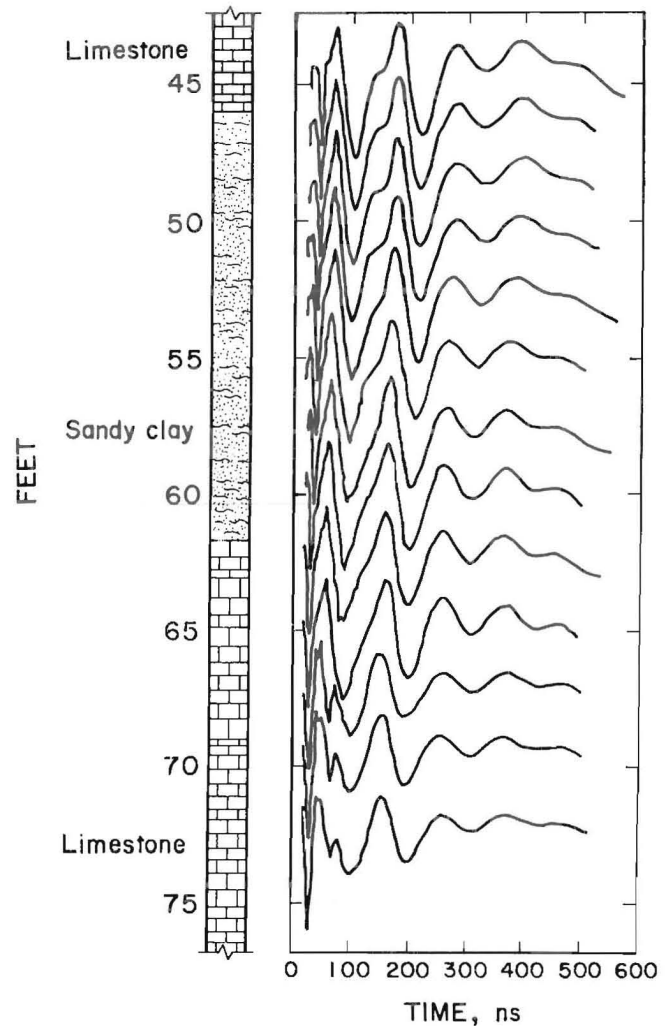


FIGURE 11. - Correlation of signatures obtained in hole H. (Note reflections at approximately 80 ns at the 63- to 71-ft depth.)

attenuated as energy is lost. The area between the dashed lines is the point at which the cavity is intersected. The horizontal distance into the cavity can be computed from the transmission speed of the EM wave through the medium. In this case the material is fine, well-indurated dolomitic limestone (fig. 11). The distance corresponds to the average depth (60 ft) to the top of the cavity intersected. From the scans (fig. 12) it appears that the reflections are increasing from 63 to 67 ft, as the probe enters into the cavity area, then decreasing from 67 to 71 ft, as the probe exits the cavity.

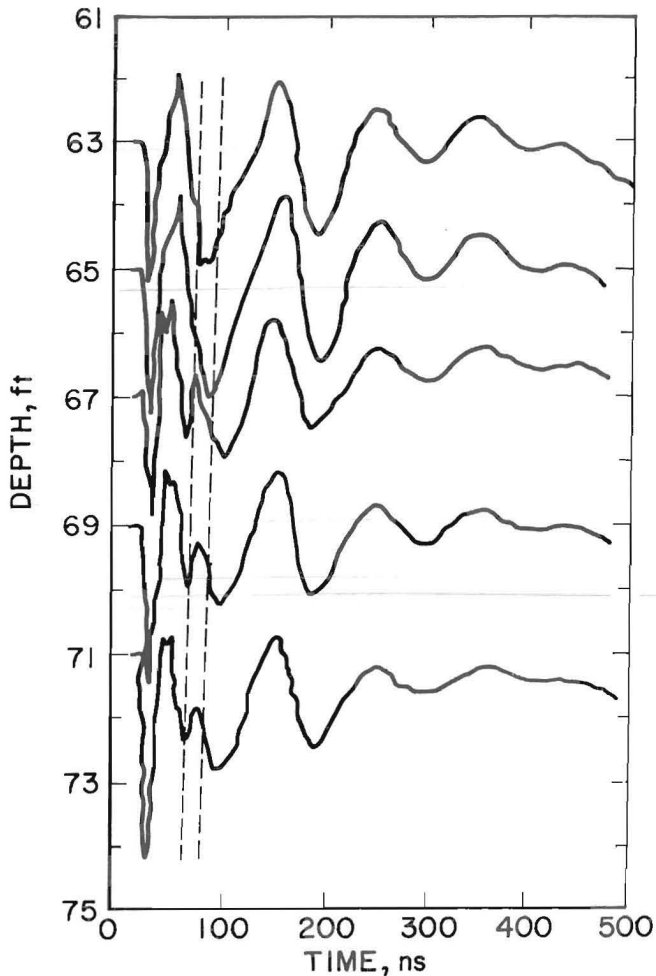


FIGURE 12. - Exploded view of radar signatures at the 63- to 71-ft depth; dashed lines denote probable intersection of cavity.

The dielectric constant of the dolomitic limestone was measured as previously described and found to be 7. The transmission speed is calculated from the equation

$$V = \frac{c}{\sqrt{\epsilon}} \text{ in ft/s,} \quad (11)$$

where V = transmission velocity, ft/s,
 c = speed of light, ft/s,

and ϵ = dielectric constant of the material;

$\therefore V = 4.0E8 \text{ ft/s} = 0.4 \text{ ft/ns.}$

Since propagation of the EM waves from the probe is based upon two-way penetration (out and return), the transmission velocity or the sampler output window distance must be halved to correspond to the received signal time frame. When the sampler output window was set at 500 ns, the calculation for the maximum distance traveled (full window) is 200 ft for two-way penetration ($0.4 \text{ ft/ns} \times 500 \text{ ns}$). Therefore, the distance to the cavity is approximately 80 ns (scaled), or 16 ft ($0.2 \text{ ft/ns} \times 80 \text{ ns}$).

Radar signatures taken in the direction of hole A failed to detect the cavity at a known maximum distance of 50 ft (hole H to hole A). Scans were taken in holes C and D but failed to detect the cavity at a maximum distance of 50 ft to the cavity.

IMAGE ENHANCEMENT

The data collected during the field testing of the subsurface probe were also analyzed using various enhancement methods. One method simply required the raw data to be plotted by the computer and a visual search made for distinct reflection. Another method required the correlation of several scans to determine the possible existence of a pattern that would indicate a return signature from the cavity area.

A third method involved taking a scan 180° from the direction desired and

subtracting the two signals, thereby leaving only the signal from the direction with the anomalous condition. This required an assumption that homogeneous material existed in all directions except for the target, and it also relied upon a precise trigger pulse. No meaningful results were obtained from this method because of these limiting factors.

The correlation method of image enhancement proved fruitful with this unit. This was the method used during the data analysis phase of the research.

SURFACE GPR UNIT

Following completion of the subsurface test with the GPR probe, a surface unit was devised to determine the propagation characteristics of the overburden. An attempt also was made to use the surface unit to delineate the underground cavity from the surface. Successful demonstration of a surface unit would prove beneficial since subsurface drilling could then be eliminated.

Figure 13 is a schematic diagram of the surface transmitter used during the testing of the aboveground unit. The 1,200-V (4,000-W) power supply circuit is shown schematically in figure 14. This power supply provides 4,000 W of pulsed power through the transmitter circuit at the same frequency range as the subsurface

probe. The direct current power supply is fed from a portable generator (5 kW). The positive and negative 600 V is fed into a pulser and timer circuit, then to the transmitter. The received signal is fed into the Tektronix 75-11 sampling unit and displayed on the Tektronix 7834 storage oscilloscope. The power supply for the surface unit is significantly larger (4X) than the borehole unit in order to improve performance and to reduce attenuation of the signal.

The system, as designed, provided a portable GPR unit suitable for field testing. The operation of the GPR was automatically controlled by the computer. A timer generated a trigger pulse that activated the nanosecond pulse generator. A synchronization pulse was applied to the sampling unit to initiate sampling. The delay between the arrival of the synchronization pulse and the time at which sampling occurred was controlled by a voltage (external sweep) that was provided by the computer. Thus, after each pulse, the sampling unit produced as an output a voltage proportional to the magnitude of one particular point on the received waveform. This value was digitalized and fed into the computer through an analog-to-digital converter (A/D). The computer then stepped the external sweep signal (and therefore the time delay) to a new value, and another point in the waveform was sampled. This process was continued until the entire waveform had been sampled point by point. In actuality, the sampling point was not changed after each pulse but the same point was sampled on a number of successive pulses. These values were averaged to eliminate noise. The number of pulses averaged was under program control and could be varied from the computer console. Usually 50 pulses were sampled and averaged at each point and 512 points were taken per scan. Approximately 3 min was required to reconstruct the complete waveform.

When the entire received waveform had been sampled, the smoothed data were recorded on either magnetic tape or disk. The smoothed waveform was also displayed on the graphic system's CRT to provide

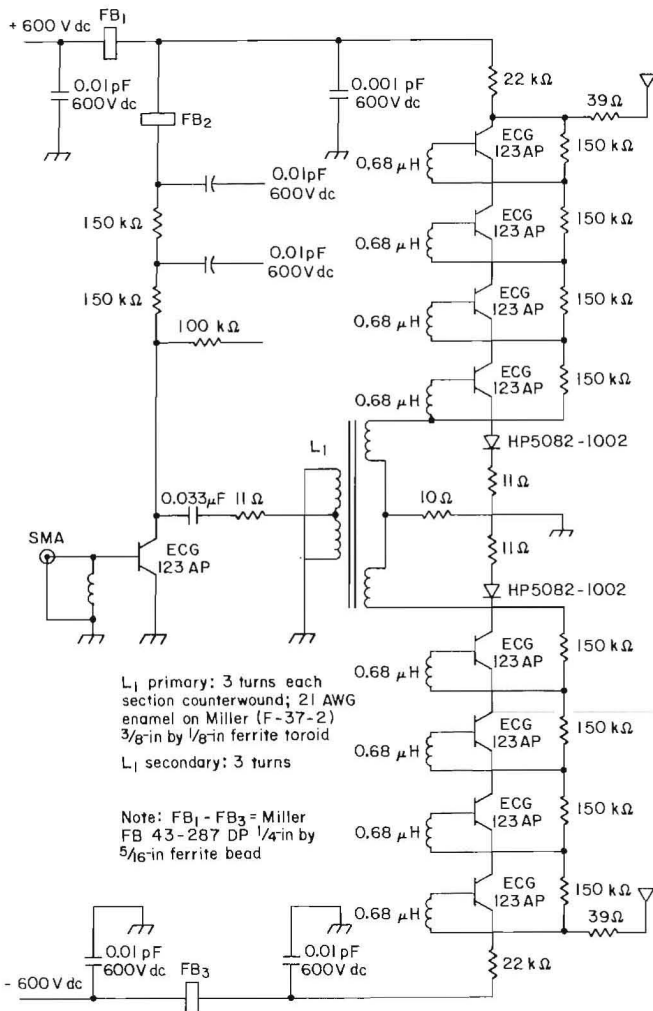


FIGURE 13. Schematic of the surface transmitter.

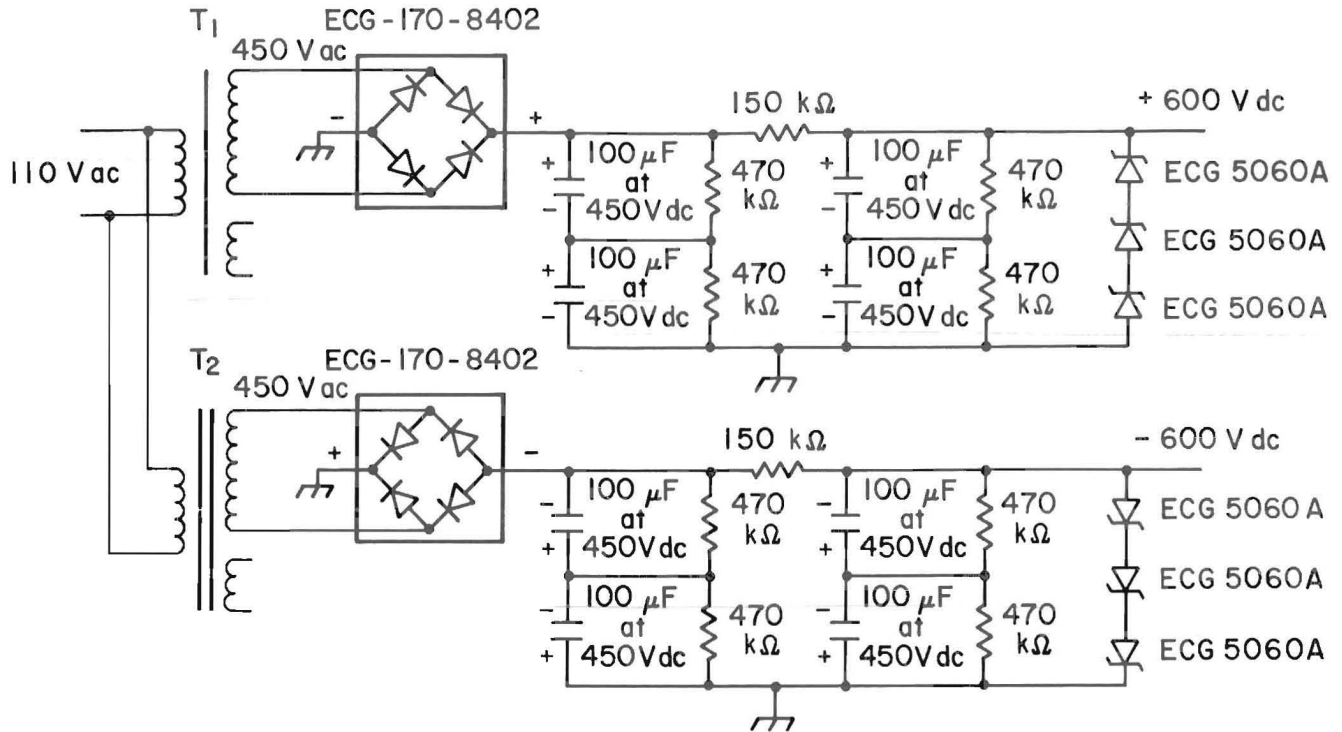


FIGURE 14. - Schematic of 4,000-W, 1,200-V power supply.

the operator with "quick look" data analysis and to allow monitoring of the system operation during each scan. A hard

copy unit gave the operator the capability to make a permanent record of the display.

SURFACE GPR TEST

The first field test of the surface GPR unit was conducted at the Mulberry site. Figure 15 shows the surface transmitter mounted on twin (dipole) antennas. The underlying plastic was used to prevent shorting of the 1,200-V (+600 V and -600 V) antennas. Figure 16 depicts the control console with 4,000-W power supply mounted inside.

Testing was conducted at hole A, where the cavity was located approximately 58 ft below the surface. The water table was measured at cavity hole A and found to be 30 ft below the surface. Figure 17A shows the result of the first radar scan over the cavity. Note the reflection near the center horizontal axis (250 ns), after which no discernible reflection occurs; this was identified to be a reflection off the top of the water-filled cavity. A reference check was made by calculating the approximate reflection point. Utilizing the data

collected from the logged hole and the electrical properties of the material, a calculation of this distance, predicting the reflection point, can be made.

Taken from table 2, the dielectric constants for the sand and clay (above and below the water table) are added to the total linear quantity (thickness) of sand and clay from the surface to the water table elevation. Below the water table the dielectric constant changes considerably.

Then

$$t_1 = \sum_{i=1}^n d_i/v_i, \quad (12)$$

where i = differences in homogeneity of material (differing strata type),

t_1 = incremental time,

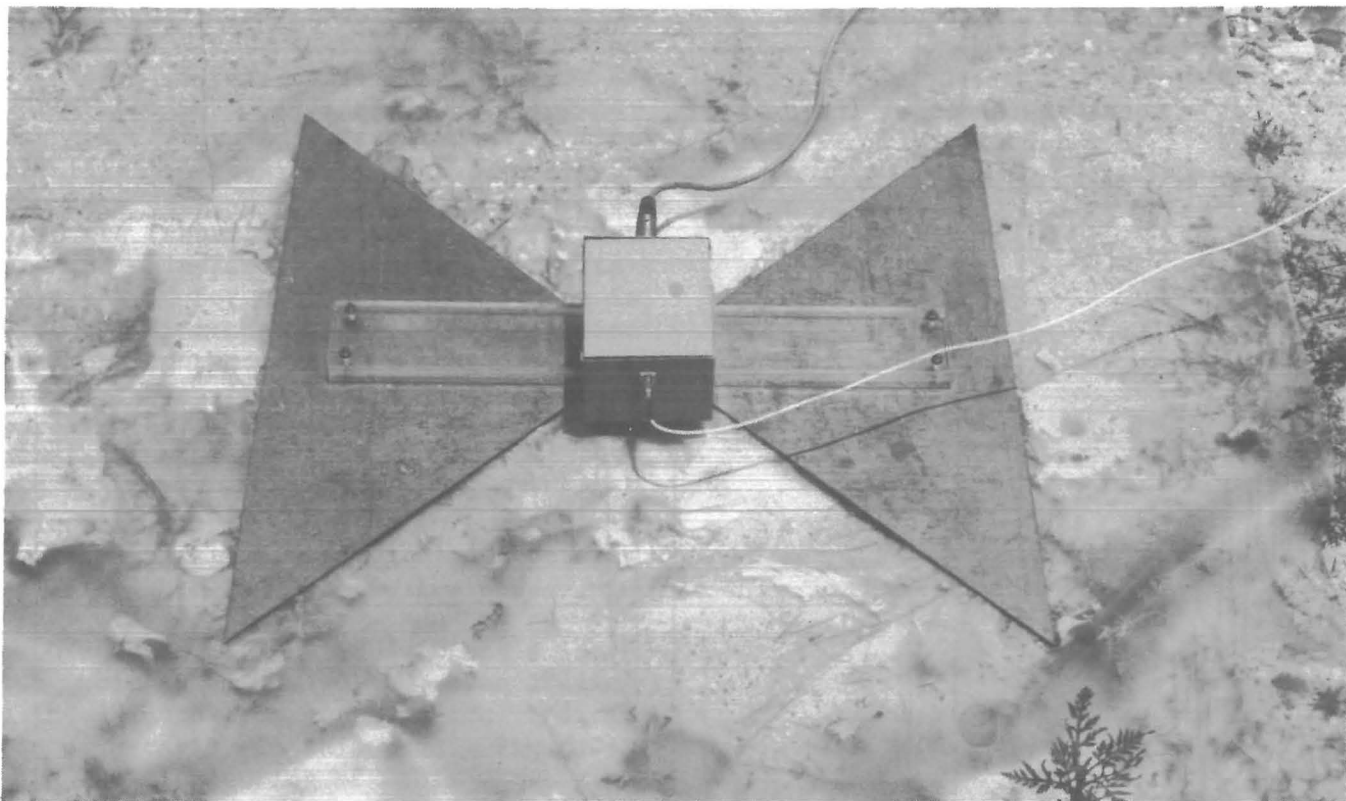


FIGURE 15. - Transmitter attached to surface dipole antenna.

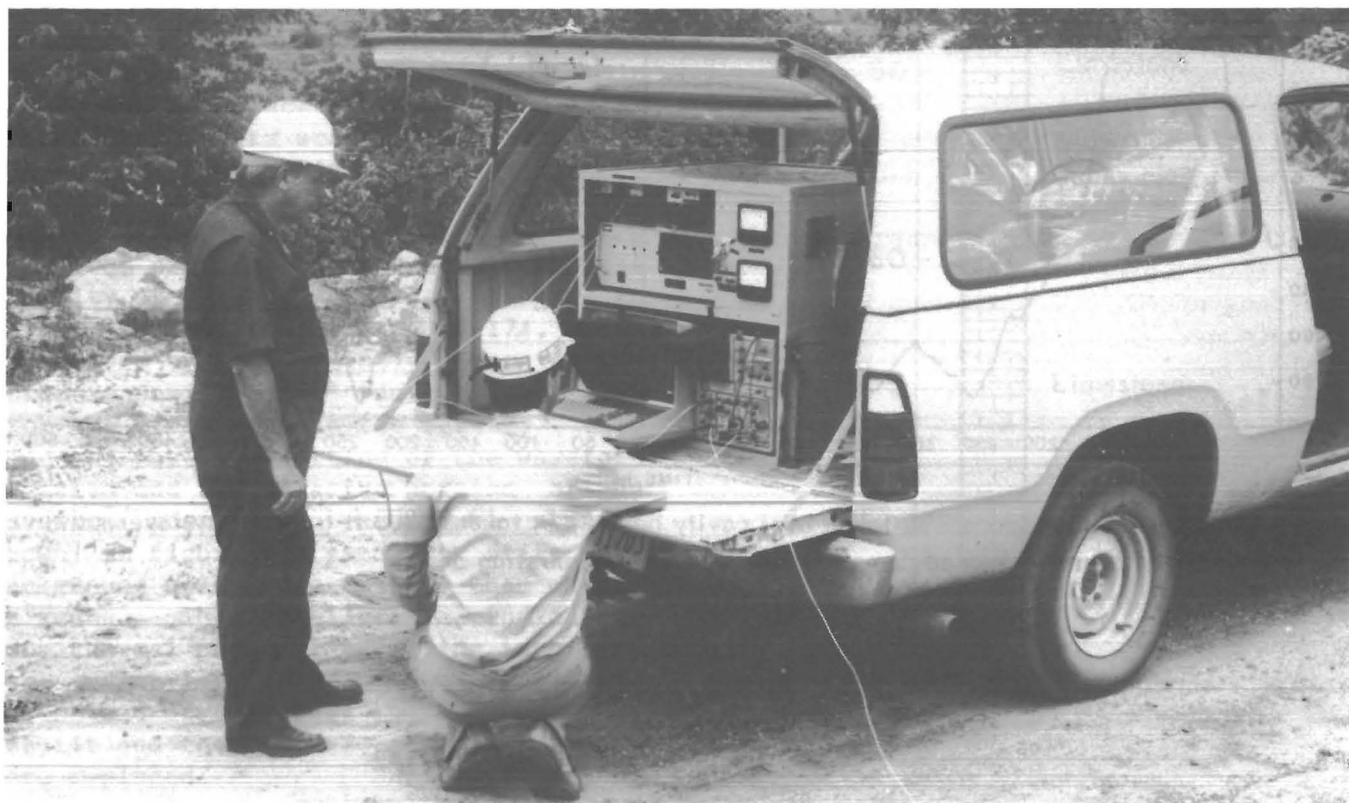


FIGURE 16. - Control console, with built-in power supply, during a field demonstration.

v = velocity of transmission,
ft/ns,

d_i = total distance per increment,
"i"; duration, ft,

where c = speed of light, ft/ns,

and ϵ_i = dielectric constant of a
strata type.

Therefore

and
$$v_i = \frac{c}{\sqrt{\epsilon_i}}, \quad (13)$$

$$t = \sum_{i=1}^n d_i / \frac{c}{\sqrt{\epsilon_i}} \cdot \quad (14)$$

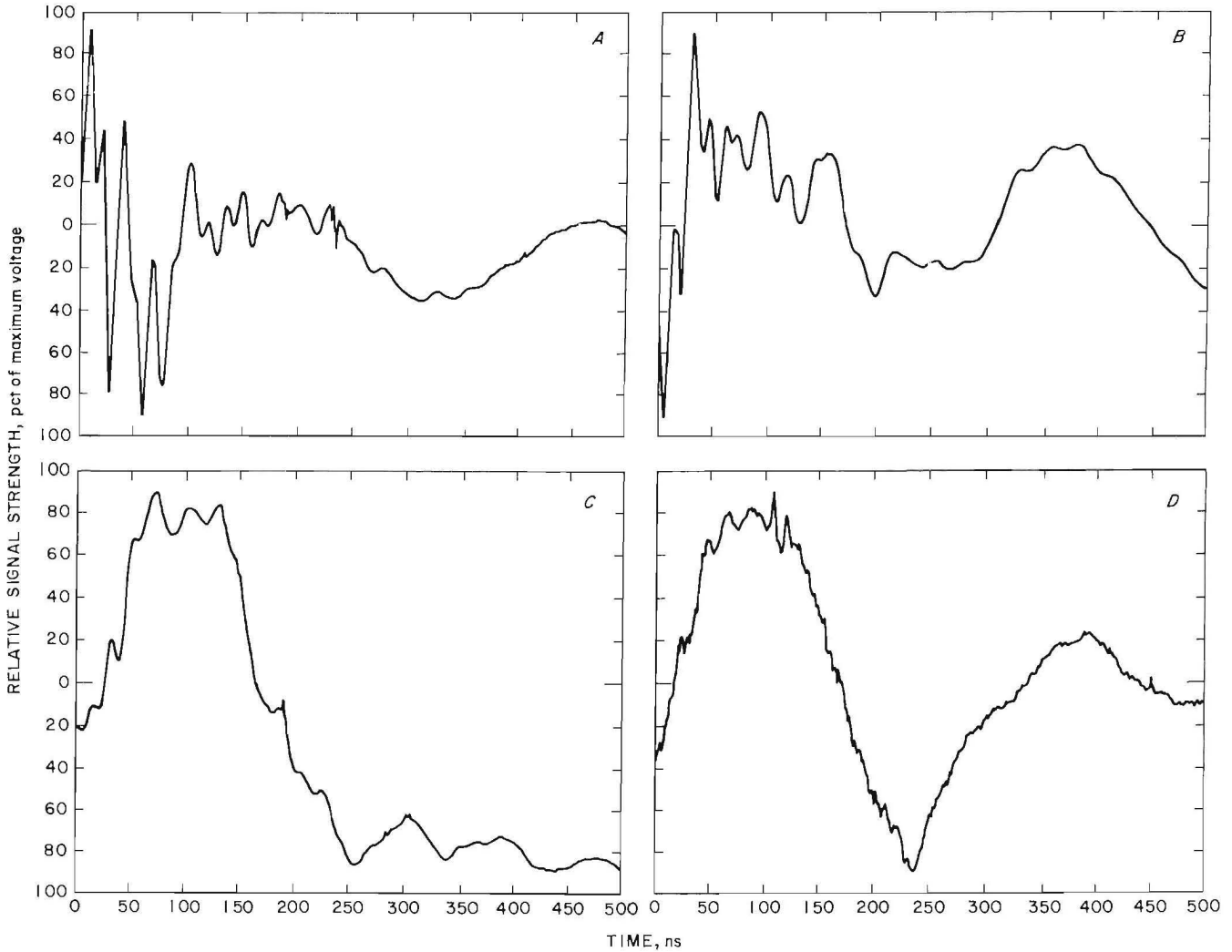


FIGURE 17. - Radar scans: *A*, taken over cavity hole *A*; *B*, taken 1,000 ft from cavity, over solid earth; *C*, taken over a proposed dams site area; *D*, taken on existing dam.

According to the indicated sources, ϵ for dry sand and clay is approximately 2.5 (14), ϵ for wet sand and clay is approximately 15 (extrapolated from tables of saturated values), and ϵ for dolomitic limerock is 7.02 (measured). From log data, d for dry sand and clay is 30 ft (above water table), d for wet sand and clay is 22 ft (below water table), and d for dolomitic limestone is 6 ft. Making the required substitution and doubling the value for two-way propagation, the cavity should be detected at approximately 300 ns, whereas the GPR detected the cavity at approximately 250 ns. A more precise knowledge of the dielectric properties of the materials should result in closer agreement between the calculated and observed values.

The GPR system was then moved due north approximately 1,000 ft to a location which previously had been drilled by IMC. There was no surface indication of a cavity in this area. Figure 18 is a lithologic log of this hole from data supplied by IMC. Figure 17B represents a radar scan taken at this location and shows no discernible reflections, which would indicate a rather large discontinuity in the material (from solid material to a void). However, certain patterns of reflections seem to match that of the cavity scan (fig. 17A), indicating some homogeneity from one site to another. This would be expected from moving the unit only a short distance from the previous site. Note that the polarity of the signals is changed in figure 17B from that of figure 17A. This was caused by inadvertently reversing the antenna position 180° during the move from the first site to the second. This made the positive portion of the waveform negative and the negative portion of the waveform positive. The signal scan as shown in figure 17B seems to drift into background noise more rapidly than earlier scans. This usually is an indication of a thermal problem developing in a system, which later proved to be the case. At the end of this test the GPR unit was rebuilt and the thermally impaired parts were replaced.

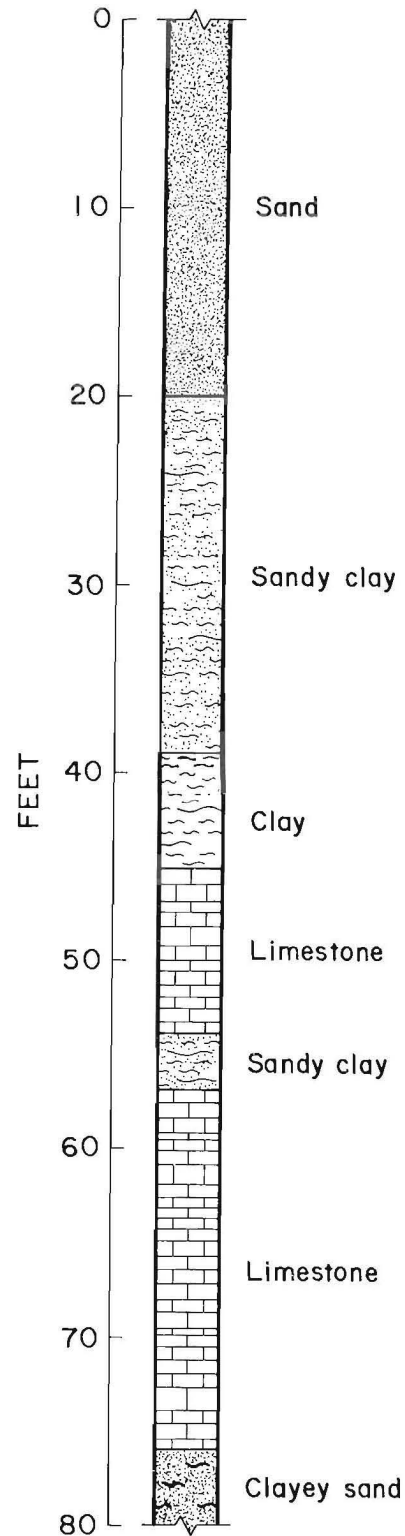


FIGURE 18.- Log of solid-ground hole approximately 1,000 ft north of cavity.

SURFACE DAMSITE TEST

The next test of the surface unit was conducted at a site approximately 3 miles northwest of Bradley Junction in Polk County, FL. This area was at a proposed damsite for IMC's Kingsford Mine. The area was adjacent to an existing impoundment and had previously been mined. The water table was approximately 10 ft below the surface. The surface material consisted of sand tailings and overburden, pushed to grade.

Based upon fully saturated sand and clay dielectric constant tables (16), the one-way propagation speed was approximately 0.2 ft/ns. The high moisture content of this unconsolidated material slowed the propagation speed significantly. The window was set at 50 ns per division, thus giving a one-way penetration distance of 10 ft per 50-ns division (0.2 ft/ns \times 50 ns per division). However, with two-way penetration this interval represents 5 ft of depth per 50-ns division.

Figure 17C is a computer-reproduced scan of the data taken at this area. Five locations were tested on 500- to 1,000-ft centers with two to four scans being taken at each location. As can be seen from the scan, the attenuation of the signal is almost complete by the time the signal has traveled 250 ns (25 ft of penetration). Also, there are no discernible reflections at this depth to

indicate the presence of a cavity. The numerous miniscule reflections along the entire length of the trace reveal certain discontinuities which would be present in a fill of heterogeneous material. If a cavity were present, a sharp and distinct reflection would be received from the rock-water interface, followed by rapid attenuation of the signal. The signal following a fully attenuated signal would then be background noise.

A scan was also taken on the adjacent dam. The dam was part of a settling impoundment used to retain the clay fines produced during the beneficiation of phosphate rock. The transmitting and receiving antennas were laid against the side of the dam, resulting in the signal being transmitted nearly 30° off the horizontal. This scan (fig. 17D) produced the results expected for the intersection of a water-filled cavity. The rapid attenuation of the signal is evident at the 250-ns (25 ft of penetration) mark, and a clear reflection of the dam-water interface was not evident. Owing to the thickness of the dam and location of the antennas, the rapid attenuation came from within the dam, possibly owing to the large water content, and not from the dam-water interface. The phreatic surface inside the dam may account for this rapid attenuation.

CONCLUSIONS

The primary conclusion to be drawn from testing of the GPR system is that meaningful structures can be identified from the data obtained. The penetration of the rock strata from the surface to a distance of 60 ft is quite significant for this initial testing of a GPR, as this is close to the average drilling depth for cavity detection. From discussions with several mining companies in the area, it was found that surface drilling is primarily limited to 50 to 100 ft for sinkhole detection.

During the tests it was found that increasing the power output of the transmitter from 1,000 to 4,000 W doubled

the transmission distance. Further increases in output power and optimization of transmitting characteristics of a GPR system should further enhance signal propagation and facilitate image interpretation.

As can be seen from figures 12 and 17A, rapid attenuation of the signal was observed at approximately 250 ns, or 50 ft of penetration. This is primarily due to the high dielectric properties of the transmission medium, which was water saturated. While system design could be modified, technical problems eliminated, and transmitter power increased, it appears that 70 or 80 ft of penetration is

the maximum estimated distance that can realistically be obtained through this saturated medium.

Finally, a considerable amount of research effort should be devoted to image enhancement. The limitations of the GPR may not lie in being able to adequately transmit the signal through the medium, but in the ability to accurately interpret the received data. Image interpretation can and should be a continuing area of improvement. Moreover, as system

performance is improved, increasingly sophisticated methods will need to be developed to interpret the perturbed signal received from the greater depths now possible, prior to total signal attenuation.

The results of these tests are encouraging enough to suggest that further research should be continued in this area prior to drawing any negative conclusions concerning the GPR in subsurface cavity detection.

REFERENCES

1. Lytle, R. J., and D. L. Lager. The Yosemite Experiments: HF Propagation Through Rock. *Radio Sci.*, v. 11, No. 4, 1976, pp. 245-252.
2. Morey, R. M. Application of Downward Looking Impulse Radar. Paper in Proceedings, 13th Annual Canadian Hydrographic Conference. Canada Centre for Inland Waters, 1974, pp. 83-99.
3. Benson, R. C., and R. A. Glaccum. Radar Surveys for Geotechnical Site Assessment. *Am. Soc. Civil Eng. Conf., Geotech. Eng. Div.* (Atlanta, GA, Oct. 23-25, 1979), ASCE Preprint 3794, pp. 1-16.
4. Wait, J. R., D. Chang, R. J. Lytle, M. A. Ralston, K. R. Umashankar, and R. C. Wittman. Analytical Bases for Electromagnetic Sensing of Coal Properties. U.S. Dep. Energy, DOE FF 8972-1, July 1978, 34 pp.
5. Ellerbruch, D. A., and J. W. Adams. Microwave Measurement of Coal Layer Thickness (contract S0144086, NBS). BuMines OFR 101-75, 1974, 33 pp.; NTIS COM 74-11643.
6. Coon, J. B., J. C. Fowler, and C. J. Schafers. Experimental Uses of Short-Pulse Radar in Coal Seams. *Geophys.*, v. 46, No. 8, 1981, pp. 1163-1168.
7. ENSCO, Inc. Mine Roof Stratigraphy Using Electromagnetic Radar (contract J0366076). U.S. Dep. Energy, DOE FE-9141-1, June 1978, 221 pp.
8. Fowler, J. C. Subsurface Reflection Profiling Using Ground-Probing Radar. *Min. Eng.* (Littleton, CO), v. 33, No. 8, 1981, pp. 1266-1270.
9. Tarantolo, P. J., Jr., and R. R. Unterberger. Radar Detection of Boreholes in Advance of Mining (Rock Salt) performance is improved, increasingly sophisticated methods will need to be developed to interpret the perturbed signal received from the greater depths now possible, prior to total signal attenuation.
10. Wu, T. T., and R. W. P. King. The Cylindrical Antenna With Nonreflecting Resistive Loading. *IEEE Trans. Antennas and Propag.*, v. AP-13, No. 5, 1965, pp. 369-373.
11. Chan, L. C., D. L. Moffatt, and L. Peters, Jr. A Characterization of Subsurface Radar Targets. *Proc. IEEE*, v. 67, No. 7, 1979, pp. 991-1000.
12. Chan, L. C., L. Peters, Jr., and D. L. Moffatt. Improved Performance of a Subsurface Radar Target Identification System Through Antenna Design. *IEEE Trans. Antennas and Propag.*, v. AP-29, No. 2, 1981, pp. 307-311.
13. Fowler, J. C. Coal Mine Hazard Detection Using Synthetic Radar (contract H0212016, XADAR Corp.). BuMines OFR 134-84, 1982, 71 pp.; NTIS PB 84-220672.
14. Westphal, W. B. Tables of Dielectric Materials - Measurements and Accuracy. Ch. in *Dielectric Materials and Applications*, ed. by A. R. Von Hippel. The MIT Press, 1954, pp. 300-314.
15. Brown, R. G., R. A. Sharpe, W. L. Hughes, and R. E. Post. *Lines, Waves, and Antennas*. Ronald Press Co., 2d ed., 1973, p. 390.
16. Suhler, S. A., and J. J. Snodgrass. In-Situ Electromagnetic Probing of Coal Seams. *Soc. Min. Eng. AIME preprint* 83-356, 1983, 10 pp.
17. Suhler, S. A., O. Tranbarger, and M. E. Converse. Development of a Deep Penetrating Borehole Geophysical Technique for Predicting Hazards Ahead of Coal Mining (contract H0252033, SW Res. Inst.). BuMines OFR 130-84, 1982, 85 pp; NTIS PB 84-239599.